UR-1360/ER40685-810
CDF/DOC/PLUG_UPGR/CDFR/2545
Version 3.0
25 July 1994

CDF Plug Upgrade Hadron Calorimeter Design

P.de Barbaro, A.Bodek, H.S.Budd, Q.Fan, P.Koehn, M.Olsson, M.Pillai,
R.C.Walker, W.K.Sakumoto, and B.Winer
University of Rochester

R.Andree, R.Bossert, R.Dixon, K.Ewald, J.Freeman, J.Grimson, J.Kerby,
P.J.Limon, F.Nobrega
Fermi National Accelerator Laboratory

C.Bromberg, J.Huston, J.P.Mansour, R.Miller, R.Richards, and C.Yousef
Michigan State University

V.Barnes, M.Fahling, A.Laasanen, J.Ross, and Q.Shen
Purdue University

1 Introduction

The upgraded plug hadron calorimeter for collider Run II is described in this document. Section 2 describes the plug calorimeter upgrade for Run II. Section 3 describes the design of the device. Section 4 details the quality assurance, quality control (QA/QC) tests used in verifying the performance of the device during construction. Section 5 gives details on the production and installation of the calorimeter components. Section 6 outlines how the energy calibration of the device can be performed. Finally, Section 7 gives the organization of manpower and responsibilities for the construction of the hadron detector.

2 The Run II Plug Calorimeter Upgrade

To cope with the shorter bunch spacing of the Tevatron upgrades for Run II, the forward (3° to 10°) and plug (10° to 38°) gas calorimeters are to be replaced with a single, compact, hermetic scintillator plate calorimeter with phototube readout [1]. The scintillator planes are constructed from smaller, optically isolated tiles that are organized into projective $\eta - \phi$ towers. Light from an individual tile in a tower is collected by a green wavelength shifting (WLS) fiber placed in a groove on the surface of a tile. Light from the WLS fiber is routed

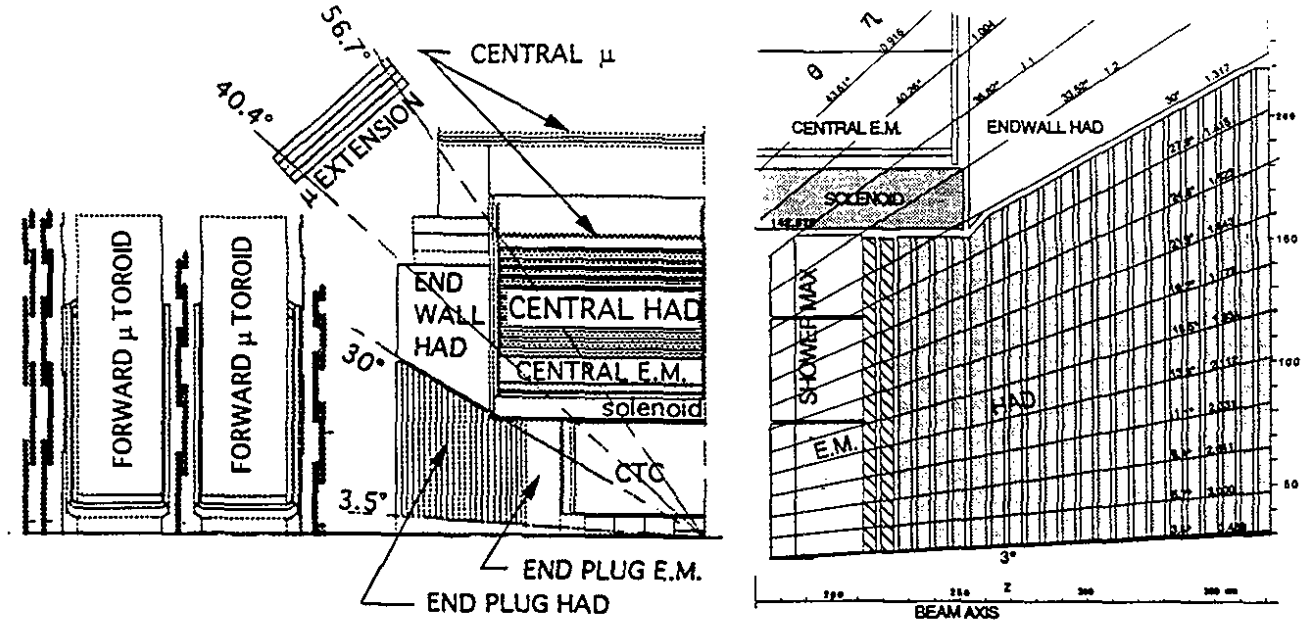

Figure 1: A quadrant cross section view of an end plug

out on its own clear transmission fiber and combined with light from the other tiles of a tower at the phototube.

The plug calorimetry upgrade preserves the gas plug calorimeter's existing steel absorber structure and leaves the solenodial magnetic field unaltered. The hadron absorber is extended to 3° by adding annular stainless steel disks to the existing plug absorber plates (see Section 5.3). In addition to removing the detector transition between the gas plug and forward calorimeters, the upgrade configuration also alleviates other detector problems. With the removal of the forward gas calorimeters, the forward muon detectors are to be moved closer towards the interaction region and thus increasing CDF's muon coverage in Run II. The upgraded plug electromagnetic calorimeter [2], being a lead/scintillator calorimeter, is denser. Since it takes up less longitudinal space, two additional stainless steel absorber plates are to be added to the front of the hadronic section of the calorimeter. Figure 1 shows a view of one upgraded end plug. These additional absorber plates have two benefits. First, there is better containment of hadron showers and reduced punchthrough into the muon detectors. In addition, they provide additional shielding in front of the projective, detector readout crack at 30°. This readout crack is unaltered by the upgrade as optical fibers from the calorimeter tiles are to be routed along this exitway to the externally mounted phototubes. The problem known as the "37° crack" (uninstrumented material in front of CEM η tower 9), is reduced by the bevel cutout of the EM calorimeter in that region.

The upgraded plug hadron calorimeter has been designed to attain the following performance. First, its $\eta - \phi$ segmentation should allow the physics topics, such b-physics, W, Z, and γ physics, and jet physics, to be done in an efficient and productive fashion. Second, it should have an energy resolution of $\sigma/E \sim (80-90)\%/\sqrt{E} \oplus 5\%$. This is dominated by

η Tower	Eng. Tile ID	η Limits	θ Limits	$\Delta\phi$
10	EM Only	1.100-1.200	33.52-36.82°	7.5°
11	17,18	1.200-1.317	30.00-33.52°	7.5°
12	15,16	1.317-1.415	27.3-30.0°	7.5°
13	13,14	1.415-1.523	24.6-27.3°	7.5°
14	11,12	1.523-1.642	21.9-24.6°	7.5°
15	9,10	1.642-1.777	19.2-21.9°	7.5°
16	7,8	1.777-1.931	16.5-19.2°	7.5°
17	5,6	1.931-2.111	13.8-16.5°	7.5°
18	4	2.111-2.331	11.1-13.8°	15°
19	3	2.331-2.611	8.4-11.1°	15°
20	2	2.611-3.000	5.7-8.4°	15°
21	1	3.000-3.643	3.0-5.7°	15°

Table 1: The nominal transverse tower segmentation of the upgraded end plug calorimeter. The tower numbering is an extension of the CHA/WHA scheme.

the sampling fluctuations from 2" steel absorber plates rather than by photostatistics. For such sampling, the calibration of the calorimeter to hadron showers is 0.1 GeV per minimum ionizing particle (mip) per tile, and the intrinsic resolution is $\sim 80\%/\sqrt{E}$. Finally, the calorimeter should be able to identify muons via their dE/dx energy loss.

The nominal transverse segmentation of the upgraded plug calorimeter is given in Table 1 and shown in Fig. 2. The segmentation of the electromagnetic (EM) and hadronic (HAD) towers are the same, with the HAD towers shadowing the EM towers. It is the result of a monte carlo study on the segmentation necessary for $e^{\pm}$ identification in $b/\bar{b}$ jets: $b \rightarrow e + X$. This is a good topology to use to tune the segmentation because the electron shower is in close proximity to a hadron jet. The monte carlo used ISAJET to generate the $b/\bar{b}$ jets and CLEOMC2 to decay the resulting $b/\bar{b}$ hadrons. In this study, the $b/\bar{b}$ hadrons were forced to decay into electrons. One electron was required to be in central region and the other in the plug. The electron tracks are marked and kept for later correlations with EM shower clusters. A simplified detector simulation was used. It included the solenodial magnetic field, the transverse EM and HAD shower shapes for transverse energy sharing into towers, and longitudinal energy sharing between the EM and HAD towers. However, resolution smearing and detector cracks and transitions were not included. A cluster finder was used to find showers in the EM compartment. For the EM cluster nearest to the electron track, electron identification cuts were applied. The cuts require that the cluster energy (E_{em}) be consisent with the electron momentum (P_e) and that the energy in the HAD towers (E_{had}) directly behind the towers in the EM cluster be consistent with that for an electromagnetic shower: $E_{em}/P_e > 0.8$ and $E_{had}/E_{em} < 0.1$. Note that charged particle tracking down to the highest η is implied here. For the segmentation of Table 1, the probability that a $b \rightarrow e + X$ electron is isolated enough to be identified by tracking and calorimetry is shown in Fig. 3.

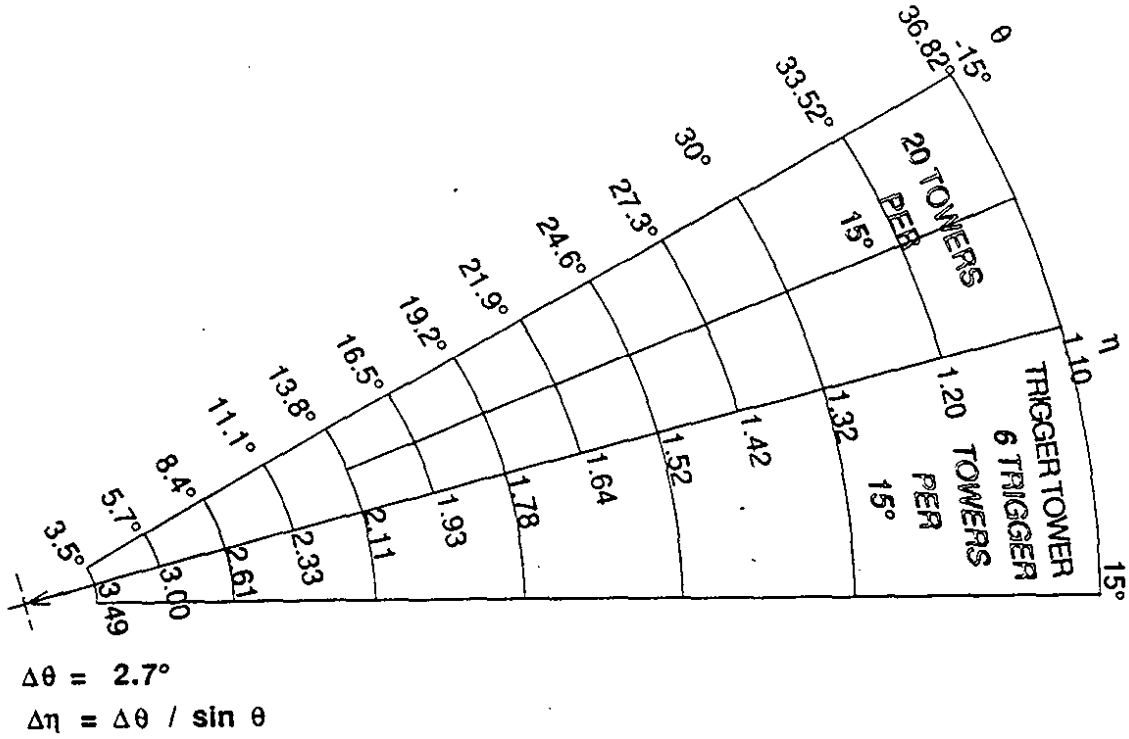

Figure 2: The segmentation in a 30° section

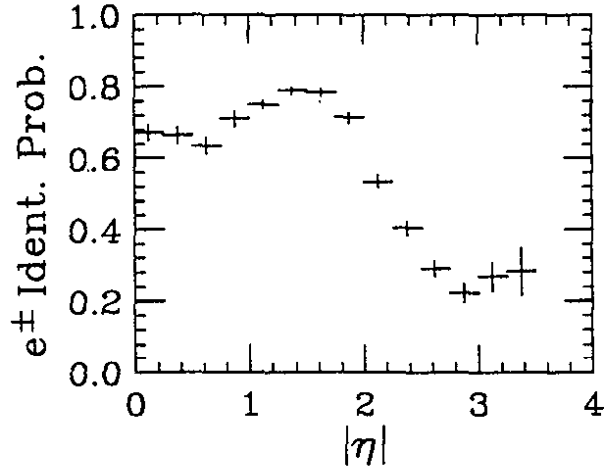

Figure 3: Identification probability for $b \to e + X$ electrons ($p_t > 5$ GeV).

The upgraded plug hadron calorimeter has 22 layers of longitudinal depth sampling. These layers are numbered from 0 to 21, with layer 0 being at the front of the calorimeter. Each layer will be instrumented with 6 mm thick Kuraray SCSN38 scintillator [3] that is read out with 0.83 mm Kuraray Y11 multiclad WLS fibers. Much R&D [1, 4, 5] has been performed in support of the design and implementation of this calorimeter. In 1991, a large, engineering prototype utilizing an earlier scintillator tile and WLS fiber technology was constructed and beam tested at Fermilab [6]. This and subsequent R&D indicate that the upgrade hadron calorimeter will attain the target energy resolution of $(80-90)\%/\sqrt{E} \oplus 5\%$. In terms of component performance, the 5% constant term requires that the variation of the tile-to-tile light yield be better than 10% and that the rms of intra-tile transverse nonuniformity be less than 4% (assuming the nonuniformity is the same for all tiles in a projective tower). An overall tile-to-tile light output variation of 10% contributes only 3% to the constant term because the hadron shower is typically spread out over more than 10 layers. R&D on prototypes and QA/QC tests on completed calorimeter counters indicate that this performance level has been met.

The individual tile light yields are more than adequate for muon detection and identification. The light yield for a tile in a completed calorimetry counter, an η tower 18 tile of layer 13, has been measured with cosmic ray muons. The cosmic ray trigger consisted of a four-fold coincidence of two small counters above and two below the layer 13 counter. The tile light yield, using a green extended phototube (Hamamatsu H1161G at 2300v), is $\sim$4 photoelectrons (*pe*) per mip. This includes the attenuation of light from a 4 m long, clear optical transmission cable (0.9mm Kuraray multiclad S-type fibers). With 22 depth layers, the total light yield for muons would be $\sim$90 *pe*'s. The cosmic ray muon pulse height spectrum is shown in Fig. 4. The photoelectron yield, $\bar{n}$, can be estimated from such spectra by either the inefficiency method or the average method. For relatively small light yields, the spectrum is approximately a smeared Poisson distribution with a mean of $\bar{n}$. Thus, the fraction of pedestal events is the Poisson inefficiency: $e^{-\bar{n}}$. In the inefficiency method, $\bar{n}$ is calculated from this fraction. This is useful at low light yields, where the spectrum is dominated by pedestal events. The ADC count to *pe* calibration can also be extracted from these low light yield spectra by dividing the spectrum mean by $\bar{n}$. In the average method, the mean of the spectrum (in ADC counts) is divided by the ADC count to *pe* calibration obtained from a low light yield calibration tile to get $\bar{n}$.

2.1 Construction Philosophy

For the tower segmentation of Table 1, there are 432 towers per endcap and a total of 17184 optically separate scintillator tiles for both endcaps. To reduce the number of individual elements, scintillator tiles from a 30° ϕ section of a longitudinal layer are constructed as a single pie-shaped mechanical unit called a "megatile". The tiles are bonded together by thin channels of opaque, white-reflective epoxy that also provide optical isolation. Readout fibers from individual tiles are routed to mass terminated optical connectors at the outer edge of the megatile on a grooved fiber routing plate (0.150" thick white, opaque polystyrene) that is secured above the scintillator. Fibers rise out of the scintillator through an oval slot in the routing plate and onto the routing grooves. The routing plate is the same size as the scintillator megatile and its use insures that the fragile optical fibers are securely held

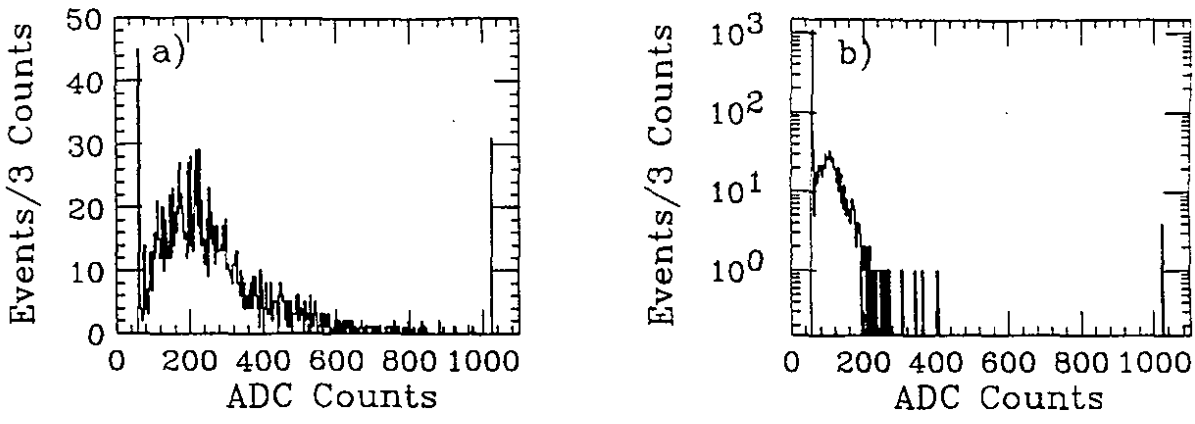

Figure 4: *Cosmic ray dE/dx spectra of 1800 events. The spike at the high end is the overflow bin, and the pedestal spike at the low end is the inefficiency (0 pe's). a) Spectrum of the layer 13 tile: 49 zeros (3.6 pe) and a mean of 212 counts above pedestal (4.2 pe). b) Spectrum of the calibration tile: 0.44 pe's (1155 zeros). The calibration is 50 ADC counts per pe: 22 counts/0.44.*

and protected. The routing plate also has grooves containing thin steel tubing channels through which a pointlike radioactive calibration source can pass over every tile. These are on the side opposite of the fiber grooves. Both the megatile and the fiber routing plate are packaged in an aluminum pan. A key feature of the design is the use of mass terminated optical connectors. Fibers in a megatile are mass terminated at the edge of the pan into an optical connector. A mass terminated optical cable transports the light from a megatile to the phototube readout. At the phototube readout, an equivalent of a cable "patch panel" assembles fibers from different longitudinal tiles of a tower onto the phototube designated for that tower.

2.2 Achieving Light Yield Uniformity

To achieve good intra-tile transverse uniformity, the tile's surface reflectivity is kept uniform and a uniform response fiber groove pattern is used. This avoids the use of a complex optical mask on the surface of the tile. To keep the tile's surface reflectivity uniform, its reflective wrapping material must be held evenly against its surface. In conjunction, tiles have a "sigma" (σ) pattern (Fig. 5) fiber groove. It is instrumented with a single loop of 0.83mm Kuraray Y11 WLS fiber whose end within the groove is mirrored. The transverse uniformity of the tiles is "tuned" by adjusting the depth of the fiber groove inside the tile. The optimal groove depth for 6 mm thick tiles is 0.100 to 0.120". At this depth, the uniformity is fairly insensitive to the placement of the fiber groove relative to a tile's edge. Figure 6 shows a response scan across a typical size tile of the calorimeter. The uniformity of individual tiles is expected to be better than 4%. To avoid long term fiber damage, the bend radius of the fibers in the grooves is kept at 1.25" (or larger). This restriction precludes σ grooves in a few towers: η tower 21 of all layers, η tower 11 of layers 1 and 2 (see Fig. 10), and η tower

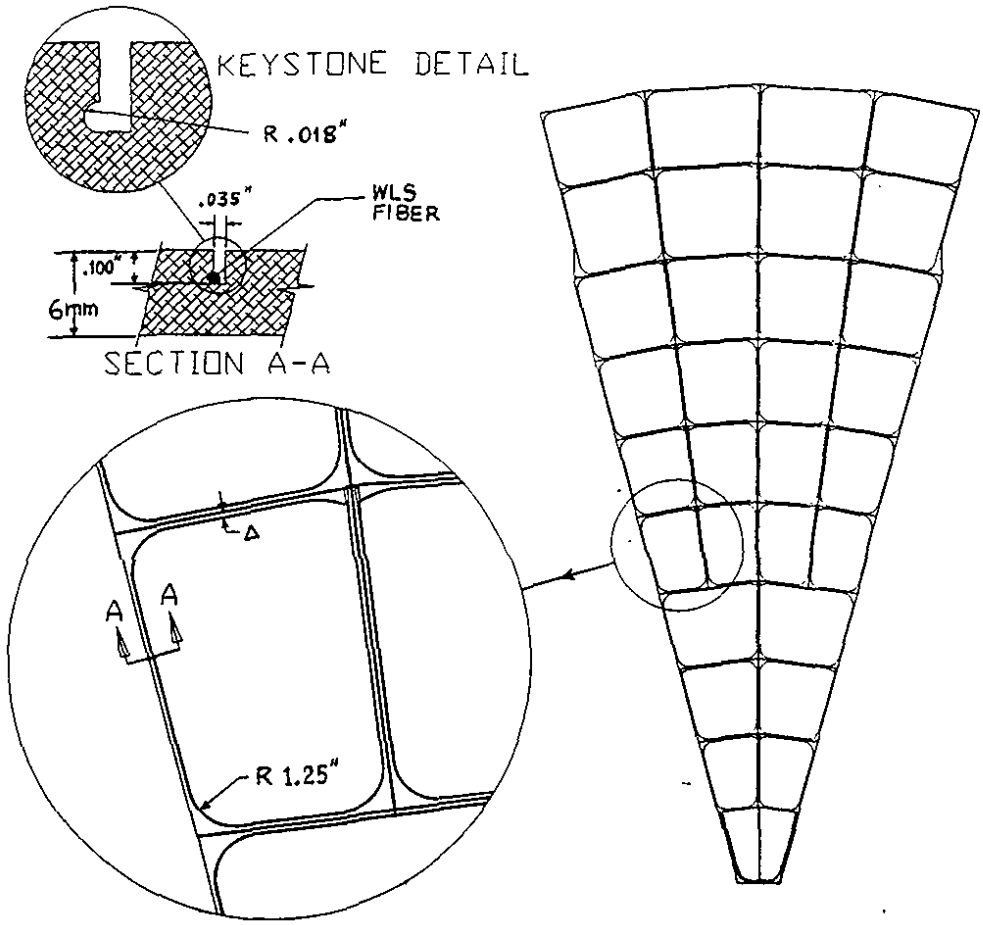

Figure 5: Fiber pattern on tiles in a 30° megatile

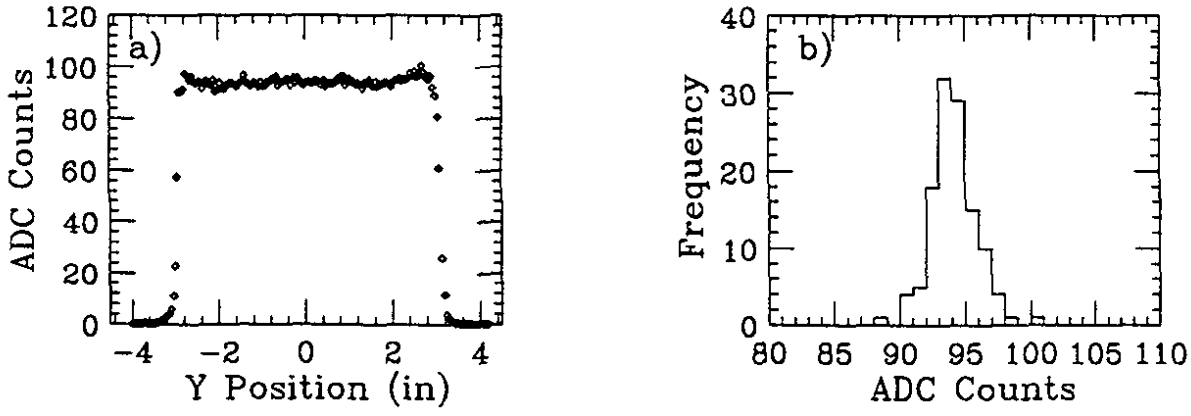

Figure 6: a) The response of a 6 mm thick SCSN38 tile with Δ =0.125" and a groove width of 0.040" and depth of 0.120" to a β-source (mip). The scan is across the center of tile. b) The distribution of responses. The mean and rms are 94.1 and 1.76 ADC counts, respectively.

12 of layer 5. There is a "J" shaped fiber groove in these tiles. For the η Tower 21 tiles, the "J" shape is flipped back and forth between even and odd layers to improve the overall tower transverse uniformity.

The light yield of tiles within a projective tower must also be kept reasonably uniform at the phototube readout. The sources of longitudinal light yield variation are given below.

1. *L/A.* Since towers are projective, the area of tiles in a tower increases from the front to the back. Larger tiles at the back have smaller light yields.
2. *Attenuation.* The length of the optical transmission cable decreases by ~60" from the front to the back. Larger tiles in the back have less light attenuated by the cable.
3. *Magnetic Field.* For SCSN38 scintillator, the 1.4 Tesla magnetic field increases the light yield by ~10% [15]. Since this field goes from full strength at the front of the tower to about zero at the back, the magnetic field boosts the light yield of the smaller front tiles.

R&D results indicate [1, 5] the light yield of the tile/fiber assemblies is approximately proportional to L/A, where L is the length of the WLS fiber embedded inside the tile and A is the tile area. Due to the projective geometry of the towers, L/A increases from the larger back tiles to the smaller front tiles by ~50%. To compensate for the increase in light from back to front, extra WLS fiber is added outside the tile on the fiber routing grooves of the white plastic cover. The light attenuation from the extra WLS fiber reduces the light yield of the smaller tiles. However, the total length of WLS fiber, both inside and outside of a tile, is kept at a fixed length for all tiles in a tower. This fixed length is the WLS fiber length of the tower's layer 21 tile. Layer 21 is the rearmost layer. In addition to the length of WLS fiber outside a tile, the other design parameter used to normalize the light yields of tiles in a tower is the length (L) of the WLS fiber in a tile. Increasing the Δ distance between the fiber and the tile's edge decreases L and decreases the light yield. Table 2 gives the expected relative light yield seen by the phototube for tiles in a layer.

3 Plug Hadron Calorimeter Design

An exploded view of a 30° section of the hadron calorimeter is shown in Figure 7. The steel absorber plates, the scintillator megatile, the fiber routing plate, and the protective aluminum pans are shown.

The actual megatile transverse segmentation is slightly different from the nominal tile segmentation given in Table 1 due to construction and engineering compromises: Fig. 2 versus Fig. 5. First of all, the scintillator tiles are trapezoidal in shape, with the corners of the trapezoid being at the corners of the $\eta - \phi$ boundaries. Between η tower 17 and 18 tiles, the 7.5° to 15° $\Delta\phi$ transition, the boundary shape is set by tower 18. At the $\theta \sim 3°$ boundary of the megatile, the edge is straight and normal to the megatile's centerline. Secondly, not all towers have full transverse and longitudinal coverage. In layers 0-5, η towers 11 or 12 do not fully cover their η boundaries. Only layers 0-2 have tiles for η tower 11 (which shadows a WHA tower). In layer 3, the coverage of η tower 11 is very small and is merged with

Table 2: Relative Light Yield for Layers

Layer Number	Δ (in)	B_{corr} (%)	Atten (%)	L/A (%)
0	0.125	9.0	-21	12
1	0.125	9.1	-20	
2	0.125	9.2	-19	
3	0.125	9.1	-18	
4	0.125	8.9	-18	
5	0.125	8.6	-17	8
6	0.125	7.9	-16	
7	0.125	7.3	-15	
8	0.125	6.4	-14	
9	0.250	5.3	-13	
10	0.250	4.4	-12	0
11	0.250	3.5	-11	
12	0.188	3.1	-9.7	
13	0.188	2.5	-8.7	
14	0.188		-7.6	
15	0.125		-6.6	-1
16	0.125	1.5	-5.5	
17	0.125		-4.4	
18	0.125		-3.4	
19	0.125		-2.2	
20	0.125	1.5	-1.1	
21	0.125	<1.0	0	0

- Layer Number: Longitudinal layer, with 0 the inner most (front) layer.
- Δ: Transverse distance of WLS fiber groove path to tile edge.
- B_{corr}: Increase in SCSN38 light yield due to the magnetic field. The absolute error is about 0.3%.
- Atten: Light attenuation in 0.9mm clear cable run from megatile connector to PMT, using $\lambda = 7.1 \pm 1.1m$.
- L/A: Change in light yield from the tile size L/A variation and compensation of the "extra" length of WLS fiber in the smaller tiles. This is from measurements using a set of tiles from η tower 18. The absolute error is about 2%.

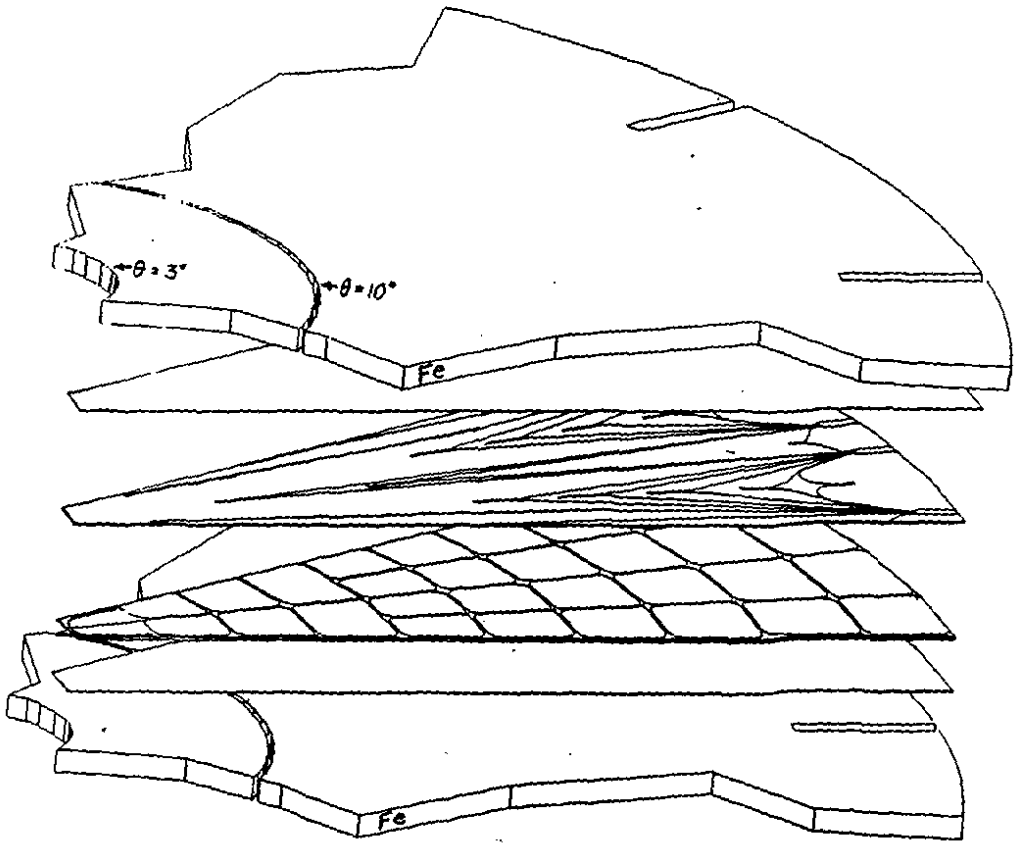

Figure 7: A 30° sector of the Hadron Calorimeter

its neighbor, η tower 12. Finally, engineering structures and tolerances slightly reduce the scintillator coverage at the boundaries of a 30° megatile. These are given in Table 3. Layer 6-21 megatiles have a notch at the outer radius region of η towers 11 and 12 to accomodate the plug's structural ribs. This notch is 1.063" wide relative to the ideal 30° ϕ boundary and runs radially from OR to "Rib IR". From "Rib IR", the notch closes up with a slope of 15°.

3.1 The Megatile Concept

The hadron calorimeter has a large number of towers: 432 per endcap. A total of 17184 tiles must be made. In order to limit the number of individual elements, the tiles from a 30° ϕ section of a longitudinal layer are grouped into a single mechanical unit called a *megatile.* A megatile has 36 (layers 0-2) or 32 (layers 3-21) tiles. The megatile along with the readout fibers are packaged in aluminum pans, called pizza pans, which are inserted into the hadron steel (see Section 5).

A cross section of the pizza pan unit is shown in Fig. 8. The unit begins with a 0.063" thick aluminum bottom cover. Then comes the 6 mm thick SCSN38 scintillator megatile covered on both sides with 0.006" thick, white, reflective Tyvek [17] paper. The surface of the scintillator tiles are grooved to hold the wavelength shifting (WLS) fibers. Above the megatile is a 0.150" thick, white polystyrene, fiber routing sheet. The fibers rise out of the scintillator through a 0.125" x 1" slot in the white plastic into grooves on the top side of the white plastic. The grooves, 0.063" wide and 0.063" deep, route the fibers to an optical connector at the outside edge of the pan. Source calibration tubes, 0.050" O.D., are placed on the bottom of the white plastic. There are four calibration tubes per megatile crossing every tile. Sheets of black, opaque Tedlar [18] are used to wrap and light tight the combined scintillator and white plastic sheets. Finally, a second 0.090" aluminum cover is located on top to provide a complete protective package. The megatile unit is held and compressed together by a set of 0.188" diameter rivets (screws), spaced apart by 18" or less. These rivets keep the inter-component gaps to ~0.015" or less. This keeps fibers from popping out of grooves and keeps the reflective Tyvek paper right against the scintillator to minimize both the tile transverse response non-uniformity and tile-to-tile light crosstalk.

3.2 Megatile Construction

The megatile is constructed from plates of 6 mm (0.236") SCSN38 scintillator. The processing of the scintillator plates is done over several steps. First, a plate with its protective paper removed from one side is positioned on the Thermwood x-y milling table. All machining operations are done on this one side only. Next, reference holes are drilled along the edges for realignment in later operations. A "long reach", 0.035" end mill is then used to cut the tower separation grooves 0.226" into the scintillator (the last 0.010" is left uncut). The scintillator plate is then removed from the milling table and the separation grooves filled with white, opaque, epoxy [7]. This is done by first taping over the grooves and then injecting epoxy into the channels [8] (see Appendix). The epoxy provides optical separation of the tiles, mechanical support, and a reflective surface at the tile edges. After the epoxy has cured, the scintillator is re-positioned on the milling table for the final machining: fiber groove routing, rivet holes, and cutting out the megatiles from the scintillator plate. The

Table 3: Megatile Engineering Boundaries

Layer Number	Z (in)	IR (in)	OR (in)	Rib IR (in)	δ_{30} (in)
0	85.875	5.323	54.125		0.063
1	88.625	5.467	54.125		0.063
2	91.375	5.611	54.875		0.063
3	94.125	5.755	54.875		0.063
4	96.875	5.899	54.875		0.063
5	99.625	6.043	54.875		0.063
6	102.875	6.213	57.088	48.125	0.125
7	105.625	6.358	59.485	49.438	0.125
8	108.375	6.502	61.078	50.719	0.125
9	111.125	6.646	62.664	52.016	0.125
10	113.875	6.790	64.250	53.313	0.125
11	116.625	6.934	65.836	54.594	0.125
12	119.375	7.078	67.422	55.891	0.125
13	122.125	7.222	69.016	57.188	0.125
14	124.875	7.366	70.602	58.496	0.125
15	127.625	7.511	72.188	59.766	0.125
16	130.375	7.655	73.774	61.047	0.125
17	133.125	7.799	75.367	62.344	0.125
18	135.875	7.943	76.953	63.641	0.125
19	138.625	8.087	78.539	64.922	0.125
20	141.375	8.231	80.125	66.219	0.125
21	144.125	8.375	81.711	67.516	0.125

- Z: Location of the scintillator plane in Z along the beam line. (Middle of gap between steel plates).
- IR/OR: Minimum/Maximum radius of scintillator from the beam line. With these IR, θ_{min} for layer 0 to 21 run from 3.54° to 3.33°.
- Rib IR: The inner radius of the plug's 1.635" wide structural support ribs in the conical region. There is a rib every 30° in ϕ.
- δ_{30}: Transverse offset distance of the megatile scintillator edges from polar lines that define its ideal 30° boundaries in ϕ.

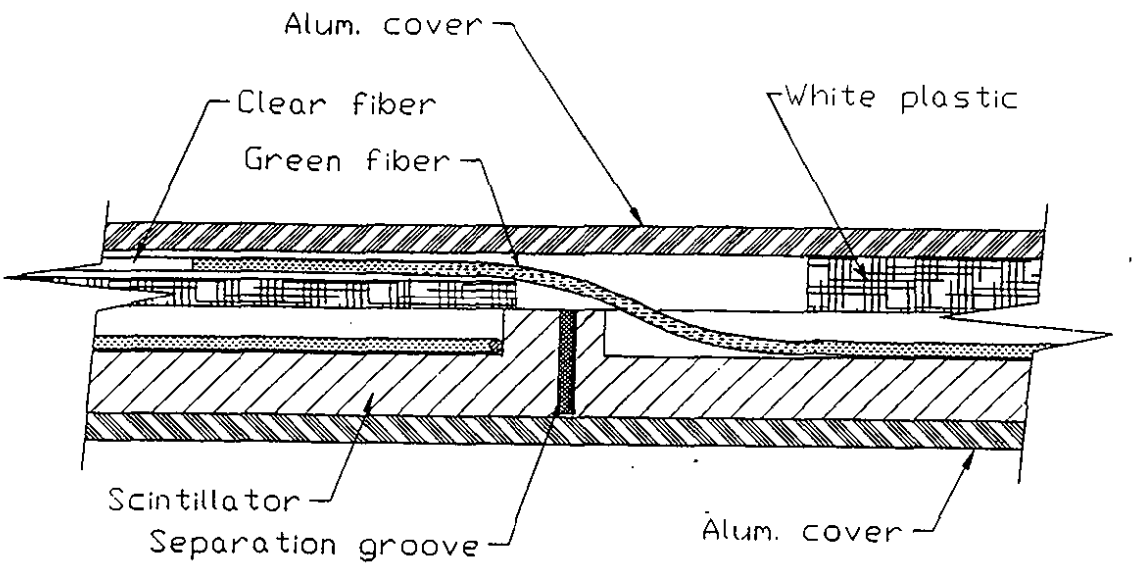

Figure 8: Hadron Pan Cross Section

0.100" deep fiber grooves are routed with a 0.035" end mill. The groove's "keystone" shape, Fig. 9, is cut with a 0.035" ball mill. The keystone helps prevent fibers from coming out of the scintillator. Finally, the megatile edges are painted with white TiO_2 paint [9] to provide a reflective surface on the outside edges of the megatile. In addition, the side of the separation groove with the leftover 0.010" of scintillator is "painted" with a black marker pen [10]. This reduces the adjacent tile crosstalk to an acceptable $1 \pm .6\%$ per side.

The construction produces a large megatile that contains individual tiles which are optically isolated but are mechanically one unit.

3.3 The Optical System

The light collected by the Kuraray Y11(250ppm) WLS fiber inside the tile is transported to the phototube using a series of clear fibers. Within the pizza pan, the fibers are Kuraray's 0.83mm multiclad, non-S type fibers. The tip of the WLS fiber inside of tiles is polished, aluminized, and protected with a thin polymer coating. The other end is spliced to a clear transmission fiber. This splice is a heat fusion splice and is covered by a 1" long, clear plastic ferrule (FEP shrink tubing, 0.05" OD) [11]. The light transmission across this splice is 92% with a 2% rms. These optical fibers are routed from the tiles to optical connectors at the edge of the megatile via grooves in the white plastic sheet. These grooves secure and protect the fibers. The grooving of the white plastic sheet is done with the Thermwood X-Y milling table. A groove pattern example is shown in Fig. 10. To avoid long term damage to the fibers, the minimum bend radius is restricted to be 1.25" or larger, and the WLS-to-clear splice is kept in a straight section of the white plastic fiber routing grooves.

At the top of the pan are four mass-terminated optical connectors. Optical cables in the form of a flat, light-tight bundle of fibers (0.9mm) carry the light from the pan's connectors

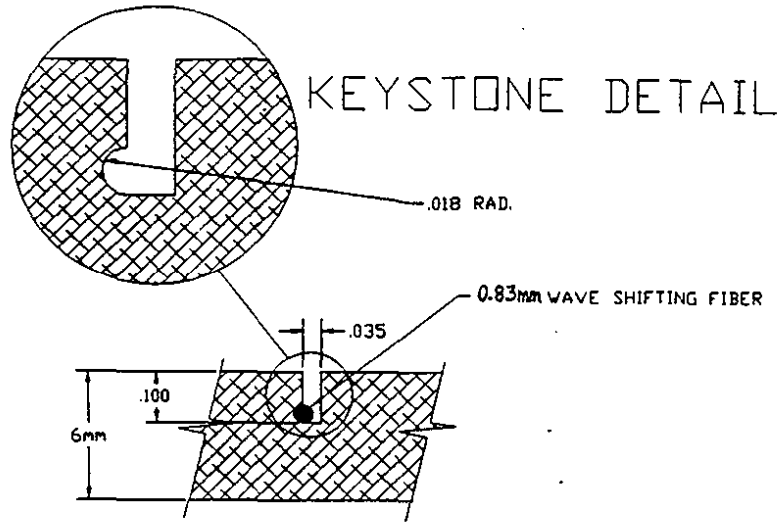

Figure 9: Cross section of the Fiber groove

to a router box near the phototubes. The cables have mass-terminated optical connectors at both ends. Within the router (fiber patch panel) box, optical signals are sorted from layers into calorimeter towers. This sorting is performed using 1mm fibers which connect fibers in layer connectors to tower based phototube light mixers. The 0.9mm and 1.0mm fibers are Kuraray, multiclad S type fibers. The use of the optical connectors allows for the segmentation of the optical path into three parts, the pizza pan, cable, and router box and provides maximum protection for the fibers at all stages of assembly and installation.

Figure 11 shows the optical connector [12]. It consists of three injection molded pieces: an outer housing and two spring loaded inserts that hold the fibers. There are different inserts for 0.83, 0.9, and 1.0mm diameter fibers. However, the fiber centers for each line up so a 0.83mm insert can be mated with a 0.9mm insert, and a 0.9mm insert can be mated with a 1.0mm insert. This permits the transition in fiber diameters at optical connections at the edge of the pizza pan (0.83 to 0.9mm) and at the router box (0.9 to 1.0mm). More light is expected to be transmitted across the connector when there is a transition from a smaller to larger fiber diameter. This also minimizes the sensitivity to light loss from insert-to-insert misalignments and tolerance variations. Insert misaligments uniformly affect all fibers of a connector, and cause 1-2% variations in light transmission. The light loss across these DDK connectors is $\sim$15%, with an rms of $\sim$3%. Tests were performed with the following combinations of prototype readout, cable, and router box fibers: (0.75 : 0.83 : 1.0mm) and (0.83 : 0.83 : 0.83mm). The results are similar in both cases and indicate that optical cables do not significantly degrade the performance of the hadron calorimeter.

The fibers and optical connectors for the pizza pans are constructed as one unit and tested before installation of the fibers into the tiles. These fiber-connector units are called pigtails. Within a pizza pan, the DDK connectors are placed on "connector trays" at the

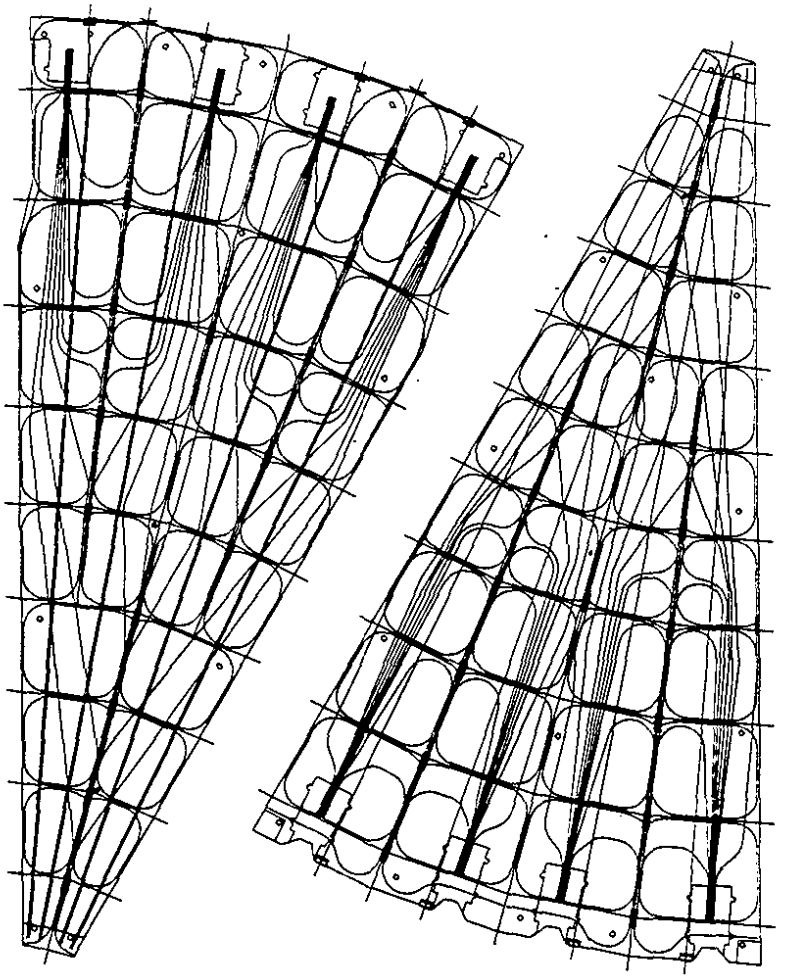

Figure 10: An overlay of the Layers 2 (right side) and 6 megatile and white plastic covers showing the Thermwood tool paths for the piece cutouts, rivet holes, separation grooves, σ-grooves, and source tube grooves and fiber routing in the white plastic. The fiber runs end at keyed, rectangular slots at the outer edge. Holding "trays" for the optical connectors fit in these slots.

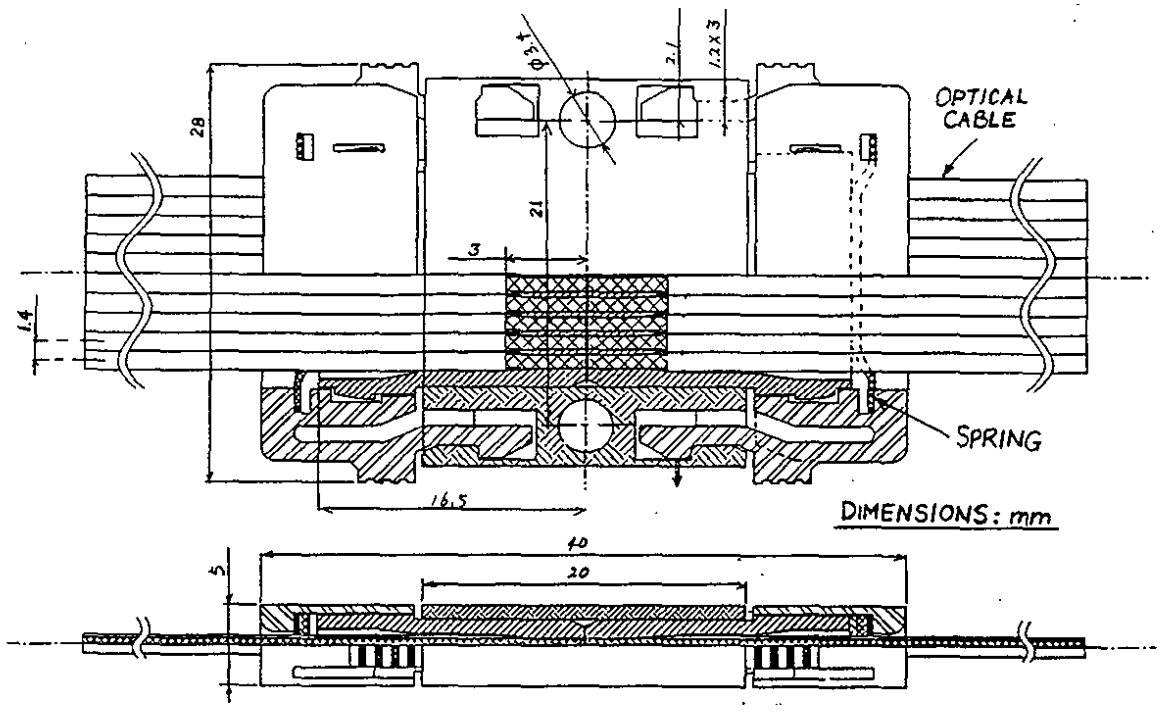

Figure 11: DDK Mass-Terminated Optical Connector

outer edge of the white plastic covers (see Fig. 10). These trays are locked in place on the cover. There are two pins on the tray that mate with two holes on the outer housing of the DDK connector and secure the connector housing to the tray and accurately position the connector insert on the fiber routing cover.

The pigtails are made using a plastic templet with fiber grooves set to the correct length of the fiber run in the actual megatile. At one end of the templet, the connector housing and insert are secured to a connector tray on the templet. The fiber holes in the DDK connector insert are matched one-to-one with the appropriate fiber grooves as they merge into the connector. First, each spliced WLS+clear fiber for a specific tower is inserted into its hole in the connector insert and then laid into its corresponding groove on the templet. As there are tick marks in the templet at the location of the splice for each fiber groove, it is clear if a fiber from a wrong tower is laid into a groove. The fibers are secured to the connector and then glued. After the glue cures, the connector insert is faced off with a diamond cutter to form a clean, uniform optical surface. The combination of the fiber fusion splice, the WLS fiber mirroring, and the optical connector produce a light transmisson rms spread of 3.5%.

3.4 Source Calibration Tubes

A radioactive Cs^{137} "wire source" (a pointlike source carried near the tip of a very long flexible wire) is used to test the megatiles immediately after construction and after installation into the plug steel. Small (0.050" OD, 0.038" ID) stainless steel tubes embedded in grooves in the white plastic are used as guides for the wire source. The grooves are 0.063" wide, 0.070" deep and on the side of the white plastic in contact with the scintillator. With this configuration, the radiation acceptance is strongly dependent on the distance of the tube away from the scintillator surface (2% per 0.10mm of separation). To minimize this

dependence, the stainless steel tubes are kept right at the surface of the white plastic. This is done by placing a strand of wooly, springy, nylon yarn on the bottom of the source tube groove, placing the stainless tube over the yarn, and then taping it over with 0.002" thick mylar tape. The combination of the yarn pushing up and the tape holding the tube down keeps the tube right at the surface of the white plastic cover.

For each pizza pan, there are 4 source tubes for local testing. They run radially from the inner to the outer edge of the pan and are spaced approximately equally apart. The tubes run approximately over the tile centers except for the radially innermost four tiles, where the tubes run approximately one-quarter and three-quarters of the way from the ϕ-edges of the tiles. At the outer edge, the tubes terminate into "funnels" which stick out a small amount from the edge of the pan. They are accessed through holes in the Al skins which surround the outer periphery of the plug's steel absorber structure. The exit points are arranged not to interfere with the optical fiber routing in the readout crack. The tubes are accessible during installation for testing purposes. During normal operation these holes (and source tubes) are covered with black tape to light tight the plug. Between collider runs when the plug is pulled out of the collider detector, the holes can be uncovered and a flexible plastic tube can be attached to the source tubes on the pans. This allows testing of all the tiles in every layer. Layers 0, 6, 12, and 19 have an additional set of 4 tubes per pan that are routed back along the steel like the optical fiber cables. This permits a radioactive source to be run into the calorimeter from the back during a collider run. Compound radiused bends are necessary to go around sharp corners. The first bend is built into the white plastic; the second bend is made in the steel extension tubes which lead to the rear plate of the calorimeter. To avoid jamming the source wire in the tube, the bend radius is kept larger than 3.5" and the interiors of all bent tubes are coated with a special lubricating paint containing graphite and molybdenum disulfide [13]. To further reduce source tube friction in the assembled calorimeter, the source-carrying "wire", which is type 304 stainless steel hypodermic tubing (needle grade fully hardened), is coated with a hard slick film containing nickel sulfide and PTFE (Nicotef coating) [14].

The four source tubes for local testing are called "straight source tubes". The additional set of tubes in layers 0, 6, 12, and 19 that are routed out for use during collider running are called "bent source tubes". The straight source tubes are special-ordered bright interior finish (8 μ-inch rms). The bent tubes have ordinary interior "K finish" (32 μ-inch rms) to provide better adhesion and durability of the anti-friction paint.

4 Testing Fixtures and Techniques

4.1 Fiber Testing

Most of the problems in the tile/fiber assembly occur from bad splices or WLS fiber problems. Therefore, fibers are checked and tested prior to use. Each batch of fiber from Kuraray is visually inspected for defects and rejected if found. For WLS fibers, a sample is scanned with UV light to assure that the light yield and attenuation length are within specifications. The fibers for each tower in a megatile are cut to length. The WLS fibers are cut in bulk, polished, and mirrored on one end. Each batch of mirrored WLS fibers has several control

fibers which are checked to assure uniformity in the mirroring.

After the WLS and clear fibers are spliced and assembled into fiber-connector assemblies (pigtails), they are individually tested. They are tested in an automated UV-scanner box that is controlled by a PC. Those that are out of specifications are either reworked, or rejected outright. The results of these pigtail scans are saved in a data base for future reference. The combined light yield and transmission distribution from these scans is shown in Fig. 12a.

4.2 Pan Testing

After installation of the optical fibers into the pan (pigtails), the megatile is put through a QA/QC test to assure that the light yields from each tile are within specifications. Light yields from tiles are required to be $\pm 20\%$ of nominal. Those that are not within specifications typically have fiber damage in either the splice or WLS fiber. The QA/QC test is there to detect and correct these problems. Light yield results from these tests are also stored in a data base for future reference. The relative tile-to-tile light yields from completed megatiles (layers 7-9) is shown in Fig. 12b. The correlations between the light yield variations measured here and the pigtail light yield variations are shown in Fig. 12c.

The light yield measurements are taken with a collimated Cs^{137} γ source positioned over the center of each tile. This is taken on an automated x-y scanning table controlled by a PC. The optical readout is similar to that used in the actual device: megatiles to mass-terminated optical cables (0.9mm) to an optical patch panel (with Hamamatsu R580-17 PMTs). The phototube gains are monitored by two systems. One is a set of reference SCSN38 tiles (read out with Kuraray Y11 fibers) permanently connected to the PMTs. These are scanned by the γ source to provide a tile/fiber reference system. The second monitor is a set of NaI (with Am^{241}) "light pulsers" directly mounted on the face of the PMTs. The megatiles, the x-y scanner table, and the optical system are within a large dark box. Measurement errors are 1% or less and the PMT gain monitoring system tracks the gain to better than 1%.

In addition to the collimated γ source measurements, pointlike source measurements are taken using the source calibration tubes and a Cs^{137} wire source. The correlation between the collimated and point source measurements is good: $\sim 1\%$ for a given size and shape of tile, indicating that the source tube locations, especially their heights above the scintillator, are very reproducible. There is a $\sim 20\%$ systematic variation of the tile response to the pointlike source as a function of tile size and shape. Large tiles have greater path lengths for the γ rays. On the other hand, the collimated γ source uses a lead cone such that the direct γ radiation falls entirely within a tile, except for the smallest tiles in some layers of η tower 21 ("tile 1"). This makes the collimated source response less dependent on source height and tile size. This is confirmed by a calculation of the volume integral of the radiation field over each tile, which indicates a 0.6% maximum tile-to-tile variation in layer 21 and a (worst case) 1.7% maximum tile to tile variation in layer 0 (excluding tile 1). The tile 1 response is down by 1.9% in layer 21, by 6.1% in layer 13, by 11.1% in layer 7, and by 17.5% in layer 0. It will be essential to validate and use these calculations to calibrate these smallest tiles relative to larger tiles, so that sourcing can accurately relate all tower responses to each other. Since only the wire source can enter the assembled calorimeter, it is essential to maintain a data base of the pointlike and collimated source responses which are contemporaneously measured during the Q/A tests.

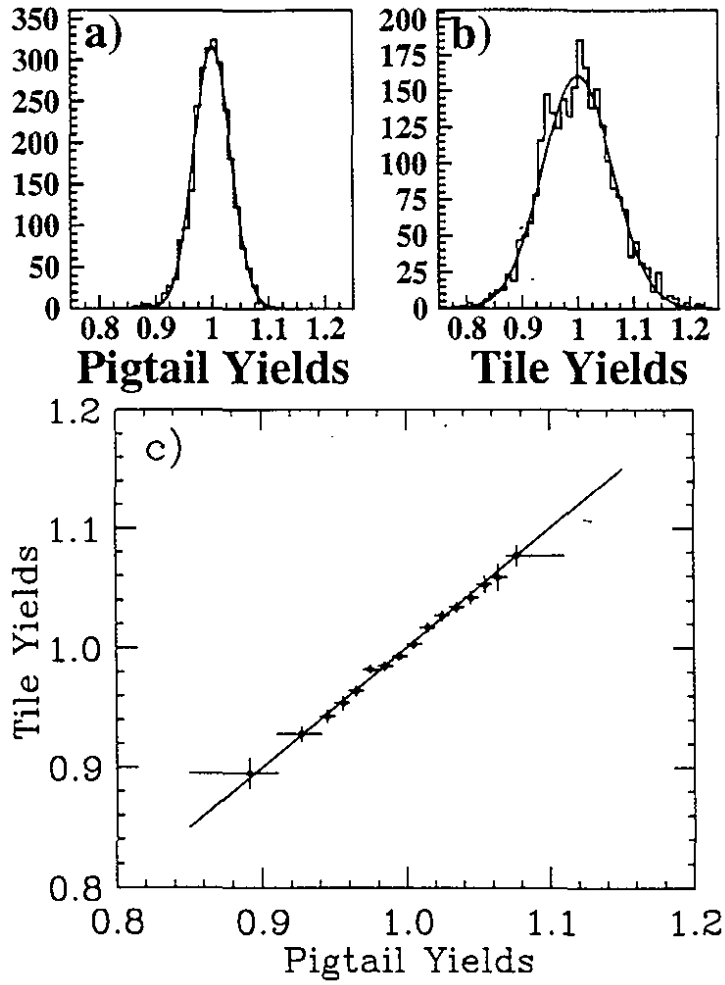

Figure 12: a) Normalized pigtail UV light yield distribution (3.5% rms), and b) normalized tile-to-tile light yield distribution (6.5% rms). Gaussian fits are superimposed. c) Correlation between pigtail and tile light yields. The line is $y = x$.

Using a similar volume integral calculation for the pointlike source responses, the calculated pointlike to collimated response ratios (averaged, for each tile, over all megatiles in a layer) track the measured ratios with a rms of better than 2%. The calculation attempts to model the actual tile geometries in detail. For the final calibrations, the use of measured ratios is preferred because they should reflect any variations in source tube placement, etc., from one megatile to another.

4.3 Summary of Quality Assurance Tests

Below are the measurements taken for quality control and quality assurance during production of the pizza pans.

1. Record information on each plate of scintillator from the manufacturer. Take and save samples as megatiles are made.
2. Measure the light yield of control samples from each batch of scintillator sheet. Measure attenuation lengths from batches.
3. Inspect each batch of optical fibers, and measure the attenuation lengths from samples of each batch.
4. Measure the combined light yield and transmission of each fiber-connector assemblies (pigtails).
5. Measure the light yield of each assembled megatile with a collimated and a wire (pointlike) Cs^{137} γ source.

The key to production quality control is contained in Steps 4 and 5. Production information kept in a data base includes:

1. The information sent from the manufacturer about the scintillator pieces.
2. Measurement of the light yield and attenuation of the scintillator control pieces.
3. The results of the UV pigtail scans.
4. The results of the collimated and wire source scan of the megatiles.

5 Production and Installation

Five hundred ninety four megatile units are needed for B0 and the test beam mock-up module (60° azimuthal coverage). There are 22 different sizes of megatiles, one for each longitudinal layer in the calorimeter. Table 4 shows the materials needed for the production.

5.1 Production

The production of the 594 megatiles is broken down into a series of tasks done in Labs 5 and 8. The milling of the scintillator and white plastic are done at the Lab 8 Thermwood facility. The megatile epoxying task is also done in Lab 8, in a production area not far from

Material	Amount
Scintillator: SCSN38 (6 mm)	600 m^2
White Plastic: HIPS [16] (3.81 mm)	600 m^2
Reflective paper: Tyvek [17] (0.15 mm)	1200 m^2
Black wrapping: Tedlar [18] (0.04 mm)	1400 m^2
Top Pizza Pan Al: 0.090" Thick	600 m^2
Bot Pizza Pan Al: 0.063" Thick	600 m^2
Y11 WLS Multiclad Fiber: 0.83 mm	17 km
Clear Multiclad Fiber: 0.83 mm	20 km
Clear 10 Fiber Cable: 0.90 mm (1.2x15mm)	4000 m
Source Calibration Tubes: SS (0.050" OD)	5600 m
Epoxy: TiO_2 loaded resin [7]	200 kg

Table 4: Summary of Materials for the of Hadron Calorimeter Construction.

the Thermwood milling machines. The aluminum pan cover customization work is done in Lab 5. The scintillator, white plastic, Tyvek and Tedlar wrapping, and the aluminum covers are partially assembled at Lab 8, put into shipment-storage boxes and then sent to Lab 5. The final assembly and testing of the megatile units are done at Lab 5. The fiber-connector assembly fabrication is a major task and is done in Lab 5. Source tube installation is done in either Lab 8 (typically) or in Lab 5, according to logistical convenience. Table 5 summarizes where each task is performed.

Two megatiles are made from a single rectangular piece of SCSN38 scintillator. This pair consists of megatiles from adjacent longitudinal layers: 0+1, 2+3, 4+5, ..., 18+19, and 20+21. The dimensions of the scintillator plates and the calorimeter layers cut from these plates are given in Table 6. For each layer, 27 megatiles are constructed. All manufacturing steps are geared to produce megatile pairs (instead of single megatiles.) There are three steps in the production of megatiles from a plate of scintillator. First, tile separation grooves are machined out. The outer boundary of the megatile is not cut, just the inner tile separation grooves. Next, the scintillator plate is taken off the milling table, the separation grooves are taped, and the epoxy is injected into the grooves. After the epoxy has cured, the plate is taken back to the milling machine and the megatiles are re-registered to the milling machines's coordinate system. Then the WLS fiber grooves are machined onto the individual tiles and alignment and structural holes are drilled into the megatiles. (The tile separation and fiber grooves are one the same side of the scintillator surface.) Finally, the megatiles are cut out of the scintillator plate.

The machining of the scintillator has been split into three steps due to several technical reasons. The milling operation requires the removal of the scintillator plate's protective paper covering on that side. Since the separation grooves are cut so that only 0.010" of material remain, the scintillator plate with separation grooves machined onto it is fragile. However, as the protective paper on the other side is left intact, it gives additional structural support to the plate when it is handled. In addition, the paper prevents surface scratching when the

Project Task	Location
White Plastic Milling	Lab 8
Scintillator Milling	Lab 8
Megatile Epoxying	Lab 8
Source Tube Installation	Lab 8/5
Megatile Pre-Assembly	Lab 8
Source Tube Preparation	Lab 5
Aluminum Pan Cutting	Vendor
Aluminum Pan Customization	Lab 5
Tyvek/Tedlar Cover Cutting	Lab 5
Fiber Preparation	Lab 5
Fiber Mirroring	Lab 7
Fiber-Connector Const	Lab 5
Megatile Final Assembly	Lab 5
Megatile Test and Storage	Lab 5

Table 5: Location of production tasks

Layers	# Size A	# Size B	# Size C
0+1	27		
2+3	27		
4+5	27		
6+7	23	4	
8+9		27	
10+11		27	
12+13		27	
14+15		27	
16+17		14	13
19+18			27
20+21			27
Total	104	126	67

Table 6: Layer Cutting Scheme. Scintillator Sizes: Size A (143cm x 100cm). Size B (178cm x 128cm), Size C (195cm x 138cm)

scintillator is moved about. The fiber grooves are not milled along with the tile separation grooves because of a risk of epoxy seeping into the fiber grooves from the separation grooves in the epoxying operation. This is because the fiber grooves can be within 3 mm of the separation grooves, and a tape seal in such a small gap is not robust.

An important quality control item in this step of the production is tracking the quality and uniformity of the scintillator plates used for each megatile. As part of the SCSN38 scintillator purchase agreement, Kuraray marked each plate delivered with an ID number that specified the production history of the plate. This information is included in the manufacturing protocol for the megatiles. Plates from different production batches are also tested and the results included in the protocol. Both the attenuation length and the light yield are monitored using tests described in the scintillator specification document. With this protocol, the megatile performance having to do with scintillator quality can easily be monitored as the megatile production proceeds.

The milling of white polystyrene plastic cover sheets and work on the aluminum cover plates are independent of the scintillator machining. However, the white plastic and aluminum cover pieces must be produced at the same pace at which the scintillator megatiles are cut. The scintillator, white plastic (polystyrene), white paper (Tyvek), light tightening wrapping (Tedlar) and aluminum covers are assembled into a partially finished megatile unit at Lab 8. This is the megatile pre-assembly step. Only the optical fibers are not part of this assembly. After this assembly, the scintillator is well protected and can be safely stored or shipped anywhere in its shipping-storage containers. After being filled, these containers are taken to Lab 5 and stored there.

An important part of the the megatile pre-assembly is the installation of the source tube calibration system onto the white plastic covers. This must be done before the optical fibers are inserted and is typically done in Lab 8 as part of the pre-assembly. The source tubes are prepared before hand in Lab 5: the stainless steel tubes are cut to length, probed for obstruction, and then crimped shut at the far end. For the straight source tubes, adaptor funnels for the wire source are glued onto the open ends. The tubes for both the straight and "bent" source tube systems are kept in their natural straight state. At curves in the source tube grooves, the tubes are put in under stress. They are not bent to shape, as this narrows and distorts the tube's cross section. Prior to laying the source tube into its white plastic cover grooves, wooly nylon yarn is layed down on the bottom of the groove to act as a spring to push up on the tube. The woolly nylon is glued to the outer edge of the white plastic and laid into the groove with an amount of stretching determined by the groove depth and length. The source tube is then laid into the groove and checked to lie between 0.006" and 0.019" above the surface of the white plastic. If it is outside these limits the nylon stretch is adjusted until the tube lies within the limits, and the nylon is glued to the other end of the groove. Then the thin, 0.002" thick and 1" wide mylar tape with acrylic adhesive is applied as flat as possible using only a roller, to avoid pushing the tube below the surface of the plastic.

At Lab 5, the fabrication of the fiber-connector assembly, the final assembly of the megatile units, and the testing of these megatile units are done. The fabrication of the fiber-connector assembly (pigtail) is a critical and major task. It involves the fiber preparation: cutting the WLS fibers to preset lengths, polishing one end, mirroring it, splicing it onto a clear fiber, and testing these fibers. It also involves the actual construction of the

pigtail: trimming the spliced fiber to a fixed length equal to the run from the end of the fiber groove inside a tile to the exit connector at the bulkhead feedthrough, potting those fibers into a mass-terminated connector, facing off and polishing the end of the connector, and QA/QC testing this. In the megatile final assembly, the top aluminum cover is removed and the four pigtails are installed. Here, the connector piece of the pigtail is put into its connector tray, the fibers in a pigtail are stuffed into their corresponding scintillator tiles, and the rest of the fiber laid and secured in its white plastic cover routing groove. Then, the top aluminum cover is put back, and the aligment and structural support rivets are screwed back together. To insure uniform compression, all rivets are torqued to fixed, specified level.

The next step is the QA/QC testing these finished megatile units. It is important to monitor the quality and uniformity of response of the individual tiles within a megatile. While the quality of the scintillator is monitored in a previous task, the quality and uniformity of a single tile is affected by other production parameters. They are: the quality of the tile separation grooves, the quality of the wrapping material next to the scintillator, and the quality of the WLS fiber groove. This is done with the collimated γ source x-y scanner. The megatiles are tested as they "come off the assembly line", and repaired if necessary.

After the megatile has passed the QA/QC test, the pan edges are light tightened with 0.003" aluminum tape. Edge sections that are subject to sliding are also taped with tough abrasion resistant tape. The pan is also gauged to assure that its thickness does not exceed 0.620". Finally, the megatile is secured and stored in a long term storage box.

5.2 Production Times

The following production times are based on simple calculations that break down complex operations into steps whose timing has been measured. The megatile count is the standard unit of production. For the Thermwood milling operations, the scintillator plate count is the production unit as two megatiles are milled simultaneously.

- *Thermwood Operations, Lab 8*
  - The production unit is a plate (SCSN38 and white polystyrene). Two megatiles are machined from one plate.
  - There are two operations here: scintillator (Sc) milling and white polystyrene (WP) milling. The maximum mill time is for the largest plate, Layer $20 \cdot 21$. The mill time decreases roughly linearly down to Layer $0 \cdot 1$, which takes about 23% less time.
  - Layer $20 \cdot 21$ mill time = 10.3 hrs = 7.6(Sc) + 2.7(WP)
  - Total time = 297 plate pairs $\times$ 10.3 hrs/plate-pair
    = 3030 Thermwood-hours

- *Megatile Epoxying and Partial Assembly: Lab 8*
  - The production unit is a megatile.
  - Timing = 8.1 man-hours/megatile

1) Aluminum pan work	35%
2) Sep. groove taping, epoxying	19%
3) White plastic - cleaning	02%
3) White plastic - source tubes	14%
4) Megatile preparation	16%
5) Partial megatile assembly	14%

- Total time = 594 megatiles × 8.1 man-hours/megatile
  = 4790 man-hours
  = 30.0 man-months

- *Megatile Final Assembly, Testing, and Storage: Lab 5*
  - The production unit is a megatile.
  - Final Assembly time = 5.0 man-hours/megatile

1) Fiber insertion	40%
2) Testing and corrective action	08%
3) Edge taping, light tightening	40%
4) Initial/final setup, storage	12%

  - Total personnel time = 594 megatile × 5.0 man-hours
    = 2950 man-hours
    = 18.5 man-months

Excluding Thermwood manpower and cutting times, the estimated "unit" construction time is 13.1 man-hours/megatile. This does not include fabrication of the fiber-connector (pigtail) assembly, which takes ~11 man-hours/megatile (with 4 pigtails per megatile). With four technicians the construction of 594 megatiles would take ~12 calendar months. The construction of the corresponding amount of pigtails in the same amount of time requires four technicians as well. Table 7 shows the overall production schedule.

5.3 Installation

The upgrade of the hadron absorber steel consists of adding two layers of 2" stainless steel disks in the cylindrical section and extending the existing steel with stainless steel washers from $\theta = 10°$ to 3°. A 0.375" thick stainless steel cone like structure at the $\theta = 3°$ edge serves as a structural load bearing member.

The scintillator hadron pan mounting scheme differs from the one used for the gas PHA, where the pan's nose is keyed on the support bars of the 10° region. The new cone structure at 3° prevents access to the small radial portion of the steel during installation. For the scintillator pans, pan aligment rods, 0.125" in diameter, are placed every 30° in azimuth at $\theta \sim 8.4°$. For all layers, they are aligned in ϕ with the outer radial support ribs of layers

Year	Jan	Feb	Mar	Apr	May	Jun	Jul	Aug	Sep	Oct	Nov	Dec
1993	PS	PS	PS	PS	PS	Fab	Fab	Fab	Fab	Fab	Fab	Fab
1994	Fab	Fab	Fab	Fab	Fab	Fab	Fab	Fab	Fab	Fab	Fab	
1995							FT	FT	FT	FT	FT	Ins
1996	Ins	Ins	Ins	Ins	Ins							R2
1997												

PS = Engineering design and Production Startup
Fab = Construction of megatiles
FT = Concurrent test beam run and steel reworking
Ins = B0 installation and checkout
R2 = Start of Collider Run II

Table 7: Schedule for the Hadron Calorimeter Construction with a 2.44 megatile per day pace. Pigtail production began in Jan94. Lab 8 operations were completed in Jun94. Fixed Target and Run II may be delayed by a year or more.

6-21. These rods serve to catch and align the nose of the pan as it is being inserted. The inner support point of the pan is the structural support cone at 3° and the alignment rods. The outer edge of the pan is supported and held at its corners by a locking, pan adjustment mechanism. This mechanism pushes on the pan's corner brackets; the radial position of the hadron pan is adjusted by adding shim to the nose piece of the pan. For layers 0-5, the adjustment mechanism is set screws through the cylindrical support ribs, while for layers 6-21, it is a set of locking, adjustment blocks mounted on the plug's radial support ribs. Since the structural support ribs of layers 0-5 go *over* the pans, those ribs above the pans must be removed during pan installation or removal. To independently hold pans when structural ribs are removed, each pan in this region has a secondary hold-down tab. This tab is at the midpoint between ribs and is secured to the outer rim of the steel absorber plates.

Once the pans are mounted in the steel, flat, mass-terminated fiber cables are connected between pans and a tester to measure its response to a source. The cable end at the pan is guided out of the steel slot by a foam support anchored to the pan. This support insures that the cable has a bend radius of at least 1" as it makes the turn to the outside of the detector. The pans and the cable are made as light-tight as possible to allow a wire source testing of the pans without having to light-tight the calorimeter structure. The wire source tests determine if the megatile and cable set is fully functional. After a pan is checked, its flat fiber cable is plugged into its router (fiber patch panel) box.

The installation involves mounting and instrumenting 528 pans. This could be done in ~3 months if both end plugs are done at the same time. Eight technicans are needed. At least 3 physicists would be involved with quality control during installation and with the shakedown. After the installation, it will probably take about 2 months to shakedown the system. During the shakedown period, technicians will be needed to fix problems. As a part of the shakedown, the aluminum skins will be put on the plug to seal and protect it. The DAQ system and phototubes will also be exercised during the shakedown period.

6 Energy Calibration

6.1 Techniques

Two calibration schemes are envisioned: muon calibration and moving radioactive source calibration. In principle, the source calibration could substitute for testbeam exposure since (a) every tile has a measured ratio of (collimated source) to (wire source), (b) the collimated source response should correlate well with either MIP response or hadron response, and (c) every tile can be wire sourced after the final optical cabling and phototubes are installed. The source calibration can be used to transfer the calibration from the testbeam to B0. However, with the magnetic field on (plugs closed), only a few layers can be sourced. These few layers can be used to determine the effect of the magnetic field on the scintillator. However, the sources cannot be used to determine the effect of the magnetic field on the hadron shower. This effect is expected to cancel since it affects the number of the particles in the steel and scintillator in the same way.

The primary calibration will in be in terms of a minimum ionizing muon signal. That is, all towers will be calibrated relative to one another using the most probable energy deposition, summed over all 22 layers, of minimum ionizing muon (defined as a MIP) and shower energies will be expressed in terms of MIPs. A preliminary calibration between MIPs and hadronic shower energy in GeV has been measured in the 1991 test beam run with the 1991 Upgrade prototype calorimeter. This calibration is only known to $\pm 5\%$ presumably because of nonuniformity in the hadron prototype tiles. The calibration, measured with 175 GeV muons, is 0.43 MIPs/GeV. It is anticipated that in the future, this calibration will be repeated with a new test beam calorimeter. Since the muons in the test beam are on average higher energy than those at B0, the energy dependence of the muon response will be checked. Previous CCFR [19] and Hanging File [20] data indicate the most probable energy deposition of muons in a calorimeter (MIP's) increases by 7% for every 100 GeV of muon energy.

By design, a muon signal has the same light yield independent of the size of the tile. Consequently, if tower-to-tower phototube gain variations are normalized to the MIP signal for a tower, the calorimeter's response to localized energy deposition anywhere (transversely and longitudinally) within it will be uniform. Because of this uniformity and relative energy calibration in terms of MIPs, each 30° pizza pan sector can be considered to be *identical* calorimeters, e.g., with identical MIP to GeV calibrations. A mockup consisting of a 60° sector of the calorimeter (two pizza pans) will be constructed in a manner identical to the actual device and placed permanently in an hadron test beam facility. This will be used to obtain the absolute calibration from MIPs to GeV as well as source response to GeV. It will also be used to study details of the performance of the device.

A radioactive wire source, pushed through the source tubes, will be used for diagnostic testing and backup calibrations. An initial calibration can be made using all layers when the plug is in the open position. When the plug is in the closed position, only a few selected layers can be monitored. The other source tubes will only be used for diagnostic purposes in case of a major problem. Note that after all towers are calibrated relative to one another, all the tiles in a pizza pan have uniform response. The radioactive source calibration can be cross-checked against calibrations using cosmic ray muons. The cosmic ray muons do

not require elaborate tracking to ensure that they remain entirely within a tower. Since the towers are identical except for the gain of the phototubes, a matrix inversion technique can be used to set the gains of the phototubes from the muon response over several towers (averaged over many events).

As the gains of phototubes do drift with time and environmental changes, the relative gain change of each individual phototube will be monitored with a laser flasher system. If the gain of a tower's phototube changes, the definition of a MIP for that tower changes and therefore it is necessary to monitor these changes to maintain the absolute energy calibration of the calorimeter. Such a system must be reproducible and stable to carry the absolute calibration from one muon calibration to another.

6.2 Electronics Requirements

The readout electronics must be able to clearly distinguish a muon signal from the noise at the low end and have a dynamic range that covers shower energies of up to 600 GeV per channel. For the ratio of the MIP signal to shower signals from the calorimeter, values from the 1991 Upgrade prototype calorimeter are used. The prototype's photoelectron yield at the peak of the muon dE/dx distribution is 35 *pe*'s/MIP/22 layers, and the hadronic shower photoelectron yield is 15 *pe*'s/GeV. Thus, the expected range ratio between a MIP and a 600 GeV shower signal is 1 to 260.

The phototubes will be operated at a nominal gain of $\sim 2 \times 10^5$. They should, however, be able to operate safely at gains up to 10^6. At a gain of 2×10^5, the integrated charge out of the PMT for a 90 *pe* MIP signal is 2.8 pC and that for a 600 GeV hadron shower is 720 pC. If the phototube signal is assumed to be a triangular pulse with a base width of 40 nsec, then the peak current for the MIP signal is 0.14 mA (7 mV into 50Ω) and 36 mA for 600 GeV of shower energy. The phototube response should be linear (within 2%) up to 36 mA (720 pC).

The ADC should have the same features as the 1992 RABBIT PMA card: a full scale of 750 pC and 16 bits of resolution. With 16 bits, the most probable value of the muon dE/dx distribution, 2.8 pC, is at 240 ADC counts. This is more than adequate for a precision calibration of the tower gain via the muon peak. The minimum acceptable is 14 bits of resolution and a full scale of 750 pC.

Another feature the new ADC should have in common with the 1992 RABBIT PMA card is the capability to digitize the average DC current simultaneously with digitizing fast pulses. This feature is essential for the radioactive source calibrations, where the pointlike source moves at 5 to 10 cm/sec and the DC phototube current must be sampled at a rate no slower than 5 Hz and preferably above 15 Hz, so as not to miss the peak in the response of each tile.

6.3 Test Beam Calibration

The mockup of the plug upgrade calorimeter at the CDF hadron test beam facility is a 60° section. Most of the steel absorber will be from the the old 60° mockup of the gas PHA. However, it will need modifications to make it identical to the planned plug upgrade configuration of the plug steel for collider Run II. Two additional 2" steel plates need to be

added to the front, and the existing steel plates need to be extended from its current angle of $\theta = 10°$ to 3°. The 2.5" thick plate at the the start of the 30° readout crack region needs to have an arc of material added to the outer radius of that plate to simulate the 45° bevel on the corresponding plate on the Collider Detector. Mounting hardware for the aluminum cover skin over the plug steel on the Collider Detector as well as the cover skin should also be duplicated for this new mockup. The steel and the layout of the support structures for 60° section mockup at the hadron test beam facility must be the same as that for the final plug upgrade design at B0.

The relative MIP calibration of the towers will be done with beam muons of a fixed momentum as was done in the 1991 test beam run. The absolute calibration of the shower energy in units of MIPs to GeV will be done using momentum analyzed hadron beams of various energies and it will require an instrumented electromagnetic shower stack to be in front of the hadronic section. This EM calorimeter must be of the same design as the actual plug upgrade EM calorimeter. Various other beam tests which study the details of its performance will also be undertaken. Results from the 1991 test beam run indicate that both a large transverse area EM and hadronic stack are needed to understand the combined response of the system to low energy hadrons (i.e., jet hadrons).

The moving radioactive source will also be used on all layers of all towers in the test beam, to verify and quantify the power of the source technique for predicting MIP and hadron shower responses. It is expected that the source technique will permit equalizing the tower responses within a few percent.

The relative calibration in MIP units must also be done on the actual calorimeter at CDF. However, the calibration at CDF must be done with the solenoidal magnetic field turned on. This is because the light yields from ionizing radiation in most scintillators increase with increasing magnetic fields [15]. In principle, any increase in light yields due to magnetic field effects will produce an increased MIP response that should compensate the corresponding increase in the hadronic shower response. Thus to first order, if the absolute calibration from MIPs to GeV is obtained from the test beam where there is no magnetic field, this absolute calibration can be transferred to CDF as long as the MIP calibration is done with the solenoid magnet on.

The magnetic field can have an additional effect. The hadron response of the CDHS iron calorimeter [21] (which is composed of magnetized steel disks in a toroidal geometry) exhibits a change of a few percent when the steel is magnetized. This is presumably due to the increased pathlength of curling low energy electrons in the magnetized steel. However, in the CDHS toroidal geometry only the steel was magnetized, and the counters were in a much lower field. In the CDF plug geometry, the magnetic field in the steel and in the scintillator is similar. Therefore, the effect is expected to cancel since the fractional increased pathlength in the iron and scintillator will be similar.

The change in scintillator response can be monitored with the radioactive source calibration by comparing the "field on" to the "field off" response. The effect is hoped to be the same for source, MIP, and hadron calibration. However, it is conceivable that the small "soft" component of the Cs^{137} excitation of the scintillator (about 5% in the geometry of the hadron megatiles) contains an electronic component which could be steered away from the scintillator by the magnetic field. We will attempt to disentangle such a possible effect from the known brightening of the scintillator in a magnetic field, by making bench top

Formulation	DER-332	DER-736	TiO_2	Jeffamine D-230
1	100	0	50	32
2	90	10	50	32

Table 8: The ratios of components and curing agent, by weight, for two formulations of TiO_2-loaded epoxy resin.

measurements using high field magnets.

7 Organization

The University of Rochester is responsible for the following items.

1. R&D for production of uniform tiles with the same gain.
2. Develop, implement, and maintain production procedures.
3. Oversee quality control, quality assurance during production.
4. Supervise detector checkout after the installation.

The fabrication of the megatile's fiber-connector (pigtail) assemblies is the responsibility of Michigan State University. The R&D and implementation of the Cs^{137} wire source calibration system are the responsibilities of Purdue University. The Upgrade Mechanical Group is responsible for the modifications to the hadron steel absorber and the installation.

8 APPENDIX: Optical Isolation of Tiles in Megatiles

In order for the megatile concept to be viable, techniques were developed to optically isolate and to form a cohesive mechanical bond between the individual tiles contained within each megatile. This section gives brief descriptions of the epoxy resin used in the megatile separation grooves, procedures and techniques to facilitate epoxy injection, techniques for epoxy injection (as well as problems associated with epoxy injection and possible solutions), and the curing procedure.

In considering resins, preference was placed on radiation hardness, material strength, stability of white pigmentation, and ease of handling. In Table 8, two formulations of TiO_2-loaded resin are given. The resin is prepared by combining base epoxy resin (Dow Corporation DER-332 and/or DER-736 epoxy resin) with TiO_2 powder (DuPont Corporation) using a ball mill. The first formulation is a short shelf-life resin comprised of pure DER-332 resin with TiO_2 powder and the second is a longer shelf-life variant consisting of a mixture of DER-332 and DER-736 resins with TiO_2 powder. Both are acceptable for the job. Once fabricated, the resins can be stored or mixed with their curing agent, Texaco Corporation Jeffamine D-230. Typically, the TiO_2 loaded epoxy is mixed with its curing agent, loaded into syringes, fast frozen in liquid N_2, and stored in a freezer at $-10°$ C for later use.

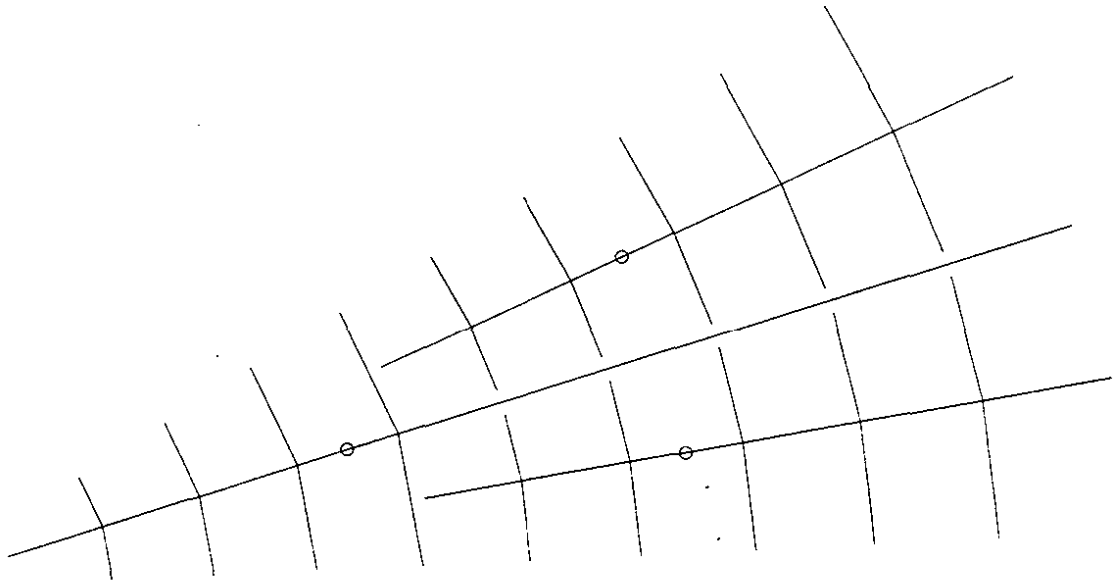

Figure 13: Separation groove layout for a megatile. The epoxy is injected into each region at points indicated by the circles.

To form the optical tile isolation strips, the tile "separation grooves" are milled almost all the way through the scintillator. A generic mill pattern is shown in Fig. 13. After the milling, the grooves are examined and blown clean with compressed air. These grooves are taped over to form covered channels through which pressurized epoxy is injected. Note that the grooves about the inner tiles have gaps of uncut scintillator which partition the megatile into three disjoint epoxy "injection" regions. These gaps are ~0.1" long and are called epoxy "dams". The separation grooves are taped with stiff, 0.003" thick kapton tape to form the epoxy flow channels. At points where four channels come together (tile corners), a piece of very thin, 0.0005" thick kapton tape cut with a razor is taped over the crossing point prior to the laying of the 0.003" thick kapton tape. The tape on the bottom must be thin and have cleanly cut straight edges so that the crease where the thin and thick tapes overlap has no air gap. Gaps must be avoided as epoxy will be sucked out of the epoxy channel through these air gaps by capillary action.

Each injection region has a central channel and arms that branch off and terminate. Air-release holes are poked through the tape at the ends of the channels to allow the escape of air displaced by the injected epoxy. With this geometry, the idea is to inject epoxy under pressure from a point along the central channel and let it flow out to the air-release holes at the ends of the channels. When a flow reaches an air-release hole, it is plugged so that the epoxy only flows towards open air-release holes. Note that there are no epoxy flow loops. This is because epoxy flow around loops cannot be controlled and often large pockets of air get trapped in them.

Final preparations made just before epoxy injection include an examination of all tape seals for possible breaches and pre-dispensing of tape for use to seal air-release holes once epoxy has filled their region or to plug possible breaches. The pre-frozen epoxy in syringes

is also heated in an oven to thaw it out and to decrease its viscosity for ease of injection.

In the injection phase, the epoxy is injected from the center of a region (see Fig. 13). The epoxy is injected out of the syringe into the separation grooves with an automated, foot-switch activated, EFD fluid dispenser [22]. The pressure setting on the EFD fluid dispenser is chosen such that injection of epoxy is carried out slowly and consistently. Ideally, this is done without stopping until the entire injection region is filled. Prolonged stoppage frequently produces large air bubbles within the epoxy channel which will need to be touched-up later. As the epoxy flow reaches each air-release hole, it is sealed with tape without stopping the epoxy flow. The flow and sealing process is continued until the entire region is filled. When leaks from inadequately sealed grooves or poorly resealed air-release holes do occur, the epoxy flow is halted until the tape seal is re-established. Once the injection is complete, the air-release holes are re-opened. The separation grooves extend ~2cm beyond the edges of the megatile. During the curing cycle, the epoxy first expands and then contracts. Re-opening air-release holes at the peripheries creates a series of pressure release points where the epoxy can expand and contract in regions outside of the megatile region. These points will be cut away when the megatiles are cut from their scintillator sheets.

The megatile sheet is room temperature cured for about day until the epoxy is no longer fluid at which time the sheet is moved to a heated, 90° F, room until fully cured (~1 day). Tape is then removed and flaws from the injection process are identified and treated. Next, the scintillator sheet receives its final machining. This includes the removal of the scintillator "dams" (separating the three epoxy injection regions of each megatile) and the cut-out of megatiles from the scintillator sheet. Finally, the outer edges of the megatile and the separation groove "dam" surfaces are covered with BC-620 white paint to complete the optical isolation of tiles within a megatile.

References

[1] G. Apollinari, P. de Barbaro, M. Mishina, et al., *CDF End Plug Calorimeter Upgrade Project*, Univ. of Rochester preprint UR-1329 (Sep93) and Fermilab FERMILAB-CONF-94-030-E (Jan94), to be published in Proceedings, 4th International Conference on the Calorimetry in High Energy Physics, La Biodola, Italy, 19-25Sep93.

[2] S.Aota et al., *A Scintillating Tile/Fiber System for the CDF Plug Upgrade EM Calorimeter*, CDF/DOC/PLUG_UPGR/CDFR/2431 (Mar94).

[3] Kuraray International Corp., New York, NY;
T. Kamon et al., Nucl. Instr. and Meth. **213** (1983) 261, *A new scintillator and wavelength shifter.*

[4] P. de Barbaro et al., *Study of Light Yield and uniformity in Hadron Calorimeters utilizing tile/fiber technology*, Univ. of Rochester preprint UR-1354 (Apr94);
P. de Barbaro et al., *Recent R&D Results on Tile/Fiber Calorimetry*, Univ. of Rochester preprint UR-1299, SDC-93-407 (Jan93);
P. de Barbaro et al., Nucl. Inst. & Meth. **A315** (1992) 317, *Research and Development Results on Scintillating Tile Fiber Calorimetry at the CDF and SDC Detectors.*

[5] P. Koehn et al., *Tile/Fiber Results for the Upgraded Plug Hadron Calorimeter*, Univ. of

Rochester preprint UR-1328 (Nov93), to be published in Proceedings of 1993 IEEE Nuclear Science Symposium and Medical Imaging Conference, San Francisco, CA, 31Oct-06Nov93.

[6] M.A. Lindgren, *The CDF Plug Calorimeter Upgrade*, in Proceedings of the Third International Conference on Calorimetry in High Energy Physics, Corpus Christi, TX, 29Sep-2Oct92, eds. P.Hale and J.Siegrist, (World Scientific, Singapore 1993), p. 61; J. Hauser et al., Nucl. Instr. & Meth. **A321** (1992) 497, *A Scintillating Fiber Detector for Electron and Photon Identification at High Luminosity Colliders*; J. Freeman et al., *The CDF Upgrade Calorimeter*, in Proceedings of the Second International Conference on Calorimetry in High Energy Physics, ed. A.Ereditato (World Scientific, Singapore 1992), p. 189.

[7] TiO_2 loaded epoxy resin: DER-332 (300g), [DER-736(30g),] TiO_2 powder (150g). The DER-736 filler is used only in layer 18-21 megatiles. "DER" epoxy resins are from Dow Chemical Company. The TiO_2 powder is either Du Pont Ti-Pure R-700 or R-900. The curing agent is Texaco's Jeffamine D-230: TiO_2 resin (100g), Jeffamine D-232 (21.33g).

[8] M.Olsson et al., *Techniques for optical isolation of megatiles*, CDF/DOC/PLUG_UPGR/CDFR/2582.

[9] Bicron BC-620 white paint, Bicron Corp, Newbury, OH.

[10] "Doubleshot" ink marker (No. 11120), Pentech International Inc., Edison, NJ.

[11] C.Bromberg et al., *A Semi-automated Splicer for Plastic Optical Fibers*, in Proceedings of the 1993 Scintillating Fiber Workshop, Notre Dame, IN, 5-12Nov93 and CDF/DOC/PLUG_UPGR/PUBLIC/2562 (Apr94).

[12] DDK Electronics, Inc., Santa Clara, CA.

[13] The lubricating paint is applied by E. M. Lubricants, Inc., Lombard, IL.

[14] The Nicotef coating is applied by Nimet Industries, Inc., South Bend, IN.

[15] J.Mainusch et al., Nucl. Instr. and Methods, **A312** (1992) 451; D.Blömker et al., Nucl. Instr. and Methods, **A311** (1992) 505.

[16] White, opaque, high impact polystyrene (HIPS) plastic sheet: silk screen grade with matte/smooth finish, and made of 100% prime ingredients. Nominal thickness of 0.150", with a tolerance of $\pm 10\%$ of nominal. Cadillac Plastic and Chemical Co., Elmhurst, IL.

[17] Du Pont Tyvek-1055B, spunbonded Olefin film. Mean thickness of 0.006" with 0.0025" rms spread. This film has a fibrous surface texture, it has high opacity, and it is very white. When used as a reflective wrapper in a SCSN38 tile/fiber counter, Tyvek-1055B has a light yield that is $\sim$20% higher relative to aluminized mylar film.

[18] Du Pont Tedlar-TCC15BL3, PVF film. Expected thickness of 0.0015"; the film is somewhat grainy with thickness of 0.002" at the bumps. Optical density ≥ 4.

[19] P. Auchincloss et al., Nucl. Inst. & Methods **A343**, 463 (1994): *A study of the energy dependence of the mean, truncated mean, and most probably energy deposition of high-energy muons in sampling calorimeters.*

[20] A. Beretras et al., Nucl. Inst. & Methods **A329**, 50, (1993): *Beam Tests of Composite Calorimeter Configurations from Reconfigurable-stack Calorimeter*;
P. de Barbaro et al., *Beam Tests of a Reconfigurable-Stack Calorimeter*, **The Fermilab Meeting DPF 92**, eds. P.H.Kasper et al. (World Scientific, Singapore, 1993) p. 1702;
P. de Barbaro, A. Bodek and B. Winer, *The Effects of Tile miscalibration on the performance of tile/fiber based hardron calorimeter*, Univ. of Rochester preprint UR-1301 (Jan93).

[21] H.Abramowicz et al. (CDHS), *The Response and Resolution of an Iron Scintillator Calorimeter for Hadronic and Electromagnetic Showers Between 10-GeV and 140-GeV*, Nucl. Instr. and Methods, **180** (1981) 429.

[22] Model 1000XL pulsed, automatic fluid dispenser and accessories. EFD Inc., East Providence, RI.